

Antitumor activity of tetrandrine citrate in human glioma U87 cells *in vitro* and *in vivo*

JINGYU SUN^{1*}, YANG ZHANG^{2*}, YONGZHAN ZHEN³, JU CUI¹, GANG HU¹ and YAJUN LIN^{1,2}

¹Key Laboratory of Geriatrics, Beijing Hospital, National Center of Gerontology; ²Peking University Fifth School of Clinical Medicine, Beijing 100730; ³Tangshan Key Laboratory for Preclinical and Basic Research on Chronic Diseases, School of Basic Medical Sciences, North China University of Science and Technology, Tangshan 063000, P.R. China

Received April 24, 2019; Accepted September 11, 2019

DOI: 10.3892/or.2019.7372

Abstract. Since the current methods of treatment for malignant glioma, radiotherapy and chemotherapy, are unsatisfactory, the development of novel therapeutic compounds is required. In the present study, the inhibitory effect of tetrandrine citrate (TetC) on the proliferation of human glioma U87 cells, as well as its mechanism of action, were investigated. An MTT assay was used to assess cell viability *in vitro*, and the production of intracellular reactive oxygen species (ROS) was determined by assessing the fluorescence intensity of 2,7-dichlorofluorescein (DCF). Flow cytometry was used to determine the level of apoptosis and cell cycle status, and the protein expression levels of apoptosis-associated proteins were determined using western blotting. Additionally, the antitumor activity of TetC was assessed *in vivo* using a nude mouse xenograft model. The results revealed that *in vitro*, the proliferative rate of U87, U251 and human umbilical vein endothelial cells (HUVECs) was significantly reduced in a dose-dependent manner following treatment with TetC, although TetC had the greatest inhibitory effect on U87 cells. The vacuolization and apoptosis of U87 cells was induced using 10 and 20 μ mol/l TetC, respectively. The overall proliferative inhibition was associated with an increase in the levels of ROS and apoptosis. In TetC-treated cells, the expression levels of apoptosis-related proteins, including cleaved (CL) caspase-3, Fas, phosphorylated (p)-p38 and p-JNK, were increased, whereas those of caspase-3 and Bcl-2 were decreased. *In vivo*, TetC was highly effective at inhibiting the growth of human glioma U87 xenografts in

BALB/c nude mice, with a percentage growth inhibition of $\geq 68.7\%$. These findings indicated that the potent antitumor activity of TetC may be mediated through an increase in ROS levels, the downregulation of Bcl-2, and the upregulation of CL caspase-3, Fas, p-p38 and p-JNK expression levels.

Introduction

According to the National Cancer Institute of United States, malignant gliomas (anaplastic astrocytoma and glioblastoma multiforme) occur more frequently than other types of primary central nervous system (CNS) tumors and account for over half of all brain cancers (1). These tumors are characterized by aggressive growth and are associated with a mean patient survival time of 12-15 months (2,3). Although the clinical application of temozolomide (TMZ) has been thoroughly demonstrated to effectively prolong the survival time of patients with brain tumors, unfortunately, glioma cells exhibit resistance to TMZ under certain conditions (4-6). Surgical resection is usually inadequate for local control, and residual tumors often lead to recurrent disease (7). Although malignant gliomas are sensitive to high doses of radiation, radiotherapeutic treatment is limited by normal tissue toxicity (8). Therefore, current therapies are unsatisfactory, indicating the requirement for novel therapeutic agents and approaches to prolong the survival time of patients with glioma.

Recently, an extensive study evaluated the safety and therapeutic efficacy of natural compounds for treating cancer. Tetrandrine (TET) is a bisbenzylisoquinoline alkaloid isolated from the root of Han-Fang-Chi (*Stephania tetrandra* S. Moore), which has been used in traditional Chinese medicine to treat arthritis (9-11), silicosis (12-14) and occlusive cardiovascular disorders (15-17) in China for several decades. TET is also reported to exert substantial inhibitory effects on various types of tumors (18-21), and to reverse multidrug resistance (22-24). Although several studies have addressed the effects of TET on gliomas (25-28), its clinical use is inconvenient due to its insolubility in water. Tetrandrine citrate (TetC), a novel TET salt, was synthesized in-house. Compared with TET, TetC has higher water solubility and can be administered by injection in an *in vivo* study. The difference between TetC and TET is only the difference in acid radicals. In the present study, the

Correspondence to: Dr Yajun Lin, Key Laboratory of Geriatrics, Beijing Hospital, National Center of Gerontology, Room 1010, Science and Education Building, 1 Dahua Road, Dongcheng, Beijing 100730, P.R. China
E-mail: linyajun2000@126.com

*Contributed equally

Key words: tetrandrine citrate, reactive oxygen species, human glioma, apoptosis, xenografts

inhibitory effect of TetC on human glioma U87 cell proliferation was investigated *in vitro* and *in vivo*, and the potential molecular mechanisms of its antitumor activity were explored.

Materials and methods

Reagents. A free base formulation of TET (purity, 98%) was purchased from Nanjing Jingzhu Biotechnology Co., Ltd., and citrate was purchased from Beijing Kehai Junzhou Biotechnology Center. TetC was synthesized in-house, and its structure is presented in Fig. 1. MTT, DMSO, NP40 and 2,7-dichlorodihydrofluorescein diacetate (DCFH-DA) were obtained from Sigma-Aldrich; Merck KGaA. All other chemicals were of standard analytical grade.

Cell culture. Human glioma U87 cells (ATCC version, glioblastoma of unknown origin) and U251 cells were purchased from the Cell Center of the Institute of Basic Medical Sciences, Chinese Academy of Medical Sciences and Peking Union Medical College (Beijing, China) and were validated by short tandem repeat DNA profiling. U87 and U251 cells were cultured in RPMI-1640 medium (Gibco; Thermo Fisher Scientific, Inc.) supplemented with 10% heat-inactivated FBS (ScienCell Research Laboratories, Inc.), 100 U/ml penicillin and 100 µg/ml streptomycin at 37°C (5% CO₂) in a humidified atmosphere. Human umbilical vein endothelial cells (HUVECs) were purchased from ScienCell Research Laboratories, Inc., and cultured in endothelial cell medium containing 100 mg/ml streptomycin, 100 IU/ml penicillin, 40 µg/ml endothelial cell growth supplement and 5% heat-inactivated FBS (all from ScienCell Research Laboratories, Inc.) at 37°C in a humidified atmosphere containing 5% CO₂. Compared with other normal cells, such as primary hepatocytes, HUVECs are easily obtained, cultured and have no characteristics of tumor cells. Thus, HUVECs were selected as normal control cells in the present study.

Cell viability assay. Cell viability assays were performed using the MTT method according to the manufacturer's instructions (Sigma-Aldrich; Merck KGaA). Cells were seeded into 96-well plates (Costar; Corning, Inc.) at a density of 4x10³ cells/well. After a 24-h incubation period, triplicate wells were treated with various concentrations of TetC (0, 5, 10, 20 and 40 µmol/l) for 48 h. Next, 20 µl MTT solution (5 mg/ml in PBS) was added to each well and incubated at 37°C for 4 h. The formazan crystals were dissolved by adding 150 µl DMSO to each well, and the absorbance was measured with a microplate reader (Multiskan™ MK3; Thermo Fisher Scientific, Inc.) at a wavelength of 570 nm. IC₅₀ values were calculated from cytotoxicity curves using the Bliss independence method (29).

Cell morphology and Hoechst staining. U87 cells were seeded at a density of 2.5x10⁵ cells/flask. Following a 24-h incubation period, the cells were treated with 0, 5, 10, 20 and 40 µmol/l TetC. After a further 48 h of treatment, images of the cells were captured using an optical microscope (x20; Olympus Corporation). The cells were then washed with pre-cooled PBS and incubated in fresh culture medium containing 10 µg/ml Hoechst 33342 fluorescent dye (Beyotime Institute

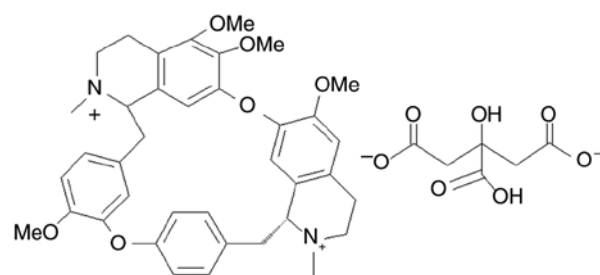


Figure 1. Chemical structure of tetrandrine citrate. The tetrandrine cation (left), and citrate anion (right).

of Biotechnology) at 37°C for 20 min. The cells were washed twice with PBS to remove residual Hoechst, and photographed using a fluorescence microscope (x20; Olympus Corporation). In addition, U87 cells were treated with 20 µmol/l TetC for 0, 1.5, 3, 6, 12, 24 and 48 h, and photographed using an optical microscope (x40; Olympus Corporation).

Detection of intracellular reactive oxygen species (ROS). Intracellular ROS measurements were performed by detecting the fluorescence intensity of 2,7-dichlorofluorescein (DCF). U87 cells in each treatment group (0, 5, 10, 20 and 40 µmol/l TetC) were incubated with the fluorescent probe DCFH-DA (1:1,000) at 37°C for 10 min in the dark, and then washed three times with ice-cold PBS. Images were acquired using an inverted fluorescence microscope (x20; Olympus Corporation), and the fluorescence intensity was detected using ImageJ software (version 1.0; National Institutes of Health). After imaging, the U87 cells were centrifuged (250 x g at 4°C for 10 min) and washed with ice-cold PBS prior to flow cytometric analysis with a FACSCalibur flow cytometer and CellQuest software (version 5.1; BD Biosciences).

FITC-Annexin V/propidium iodide (PI) apoptosis analysis. Cells were seeded at a density of 2.5x10⁵ cells/flask and incubated for 24 h at 37°C (5% CO₂), prior to treatment with 0, 5, 10, 20 or 40 µmol/l TetC. After 48 h, the cells were collected and resuspended in 200 µl binding buffer; 10 µl FITC-labeled enhanced Annexin V and 10 µl PI were added and the samples were gently mixed. After incubation in the dark for 15 min at room temperature, the samples were diluted with 300 µl binding buffer and subjected to flow cytometric analysis using the FACSCalibur flow cytometer with CellQuest software (version 5.1; BD Biosciences).

Cell cycle assay. To determine the effect of TetC on cell cycle progression, cells were cultured for 6 h (one cell cycle) in medium containing 0, 5, 10, 20 or 40 µmol/l TetC. The cells were washed with PBS, collected by trypsinization, fixed with 70% ethanol and treated with 1% NP40 and 5 mg/ml RNase for 30 min. After staining with 50 mmol/l PI, the cells were subjected to flow cytometric analysis as aforementioned.

Western blotting. Cells were harvested and washed with PBS, and whole-cell extracts were prepared by incubating the cells on ice in lysis buffer containing phosphatase inhibitor cocktail (Roche Diagnostics). The lysates were clarified by centrifugation (12,000 x g at 4°C for 20 min),

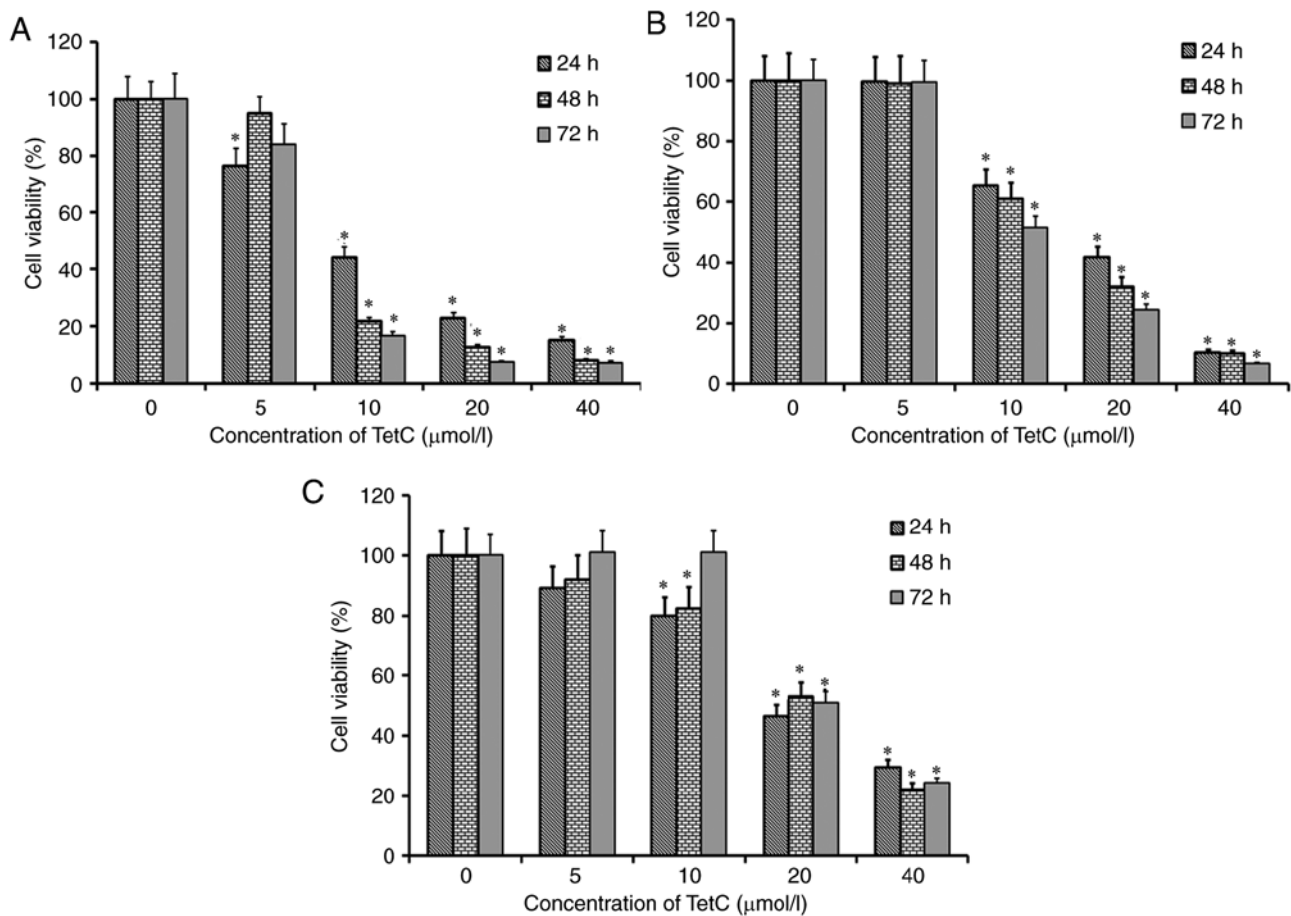


Figure 2. Inhibition of human glioma U87 cells, U251 cells and HUVECs proliferation by TetC. U87 cells (A), U251 cells (B) and HUVECs (C) were exposed to 0, 5, 10, 20 and 40 $\mu\text{mol/l}$ TetC for 24, 48 and 72 h, and the proliferative rate was determined using an MTT assay (three replicates). * $P < 0.05$, compared with the control group. TetC, tetrandrine citrate.

and the total protein was quantified using a BCA Protein Assay kit (Pierce; Thermo Fisher Scientific, Inc.). Equal amounts of lysate (40 $\mu\text{g/lane}$) were resolved by 10% SDS-PAGE and transferred to polyvinylidene difluoride membranes (EMD Millipore). The membranes were blocked in Tris-buffered saline with Tween-20 (TBST) containing 5% skim milk at room temperature for 2 h, and incubated with the corresponding primary antibodies at 4°C overnight. The membranes were then incubated with horseradish peroxidase-conjugated secondary antibodies for 1 h at room temperature. All primary antibodies were purchased from Cell Signaling Technology, Inc., and were targeted against cleaved (CL) caspase-3 (cat. no. 9661; 1:1,000), caspase-3 (cat. no. 9662; 1:1,000), Fas (cat. no. 8023; 1:1,000), Bcl-2 (cat. no. 15071; 1:1,000), Bax (cat. no. 2772; 1:1,000), p-p38 (cat. no. 9216; 1:1,000), p38 (cat. no. 9212; 1:1,000), p-JNK (cat. no. 9255; 1:1,000), JNK (cat. no. 9252; 1:1,000) and β -actin (cat. no. 8457; 1:1,000). β -actin was used as the endogenous reference protein. Secondary antibodies against rabbit (cat. no. 7074; 1:5,000) or mouse (cat. no. 7076; 1:5,000 dilution) IgG were also purchased from Cell Signaling Technology, Inc., and the pre-stained protein marker p7708V was purchased from New England BioLabs, Inc. The proteins were visualized using enhanced chemiluminescence western blotting detection reagents (GE Healthcare). ImageJ software (version 1.0;

NIH) was used to quantify the optical density for treated samples, which were normalized to the β -actin internal controls.

In vivo assessment of the therapeutic effects of TetC in BALB/c nude mice. A total of 14 female BALB/c nude mice (20 \pm 2 g) aged 4-6 weeks were obtained from Vital River Laboratories Co., Ltd., and used to create a human glioma U87 xenograft model. The mice were maintained in a temperature-controlled room (22 \pm 2°C) with a 12-h light/12-h dark cycle and a relative humidity of 40-60%, with *ad libitum* access to food and water. All animal experiments were approved by the Institutional Animal Care and Use Committee of Beijing Hospital, and the U87 xenograft mouse model was established as previously described (30). Briefly, U87 cells (5 \times 10⁶ cells per animal) were injected into the armpit of each mouse. When the tumor volume had reached a volume of 1 cm³, it was removed and cut into 2 mm³ pieces; these tissues were inoculated into the armpits of another group of female nude mice. After 3 days of tumor growth, the animals were randomly divided into the control or 200 mg/kg TetC (22 g/l)-treated groups (six mice per group). Each animal received either 200 μl PBS (vehicle control) or TetC via intraperitoneal injection, every other day for 14 days. Health status and behavior of mice were monitored daily. At the end of the experiment, the mice

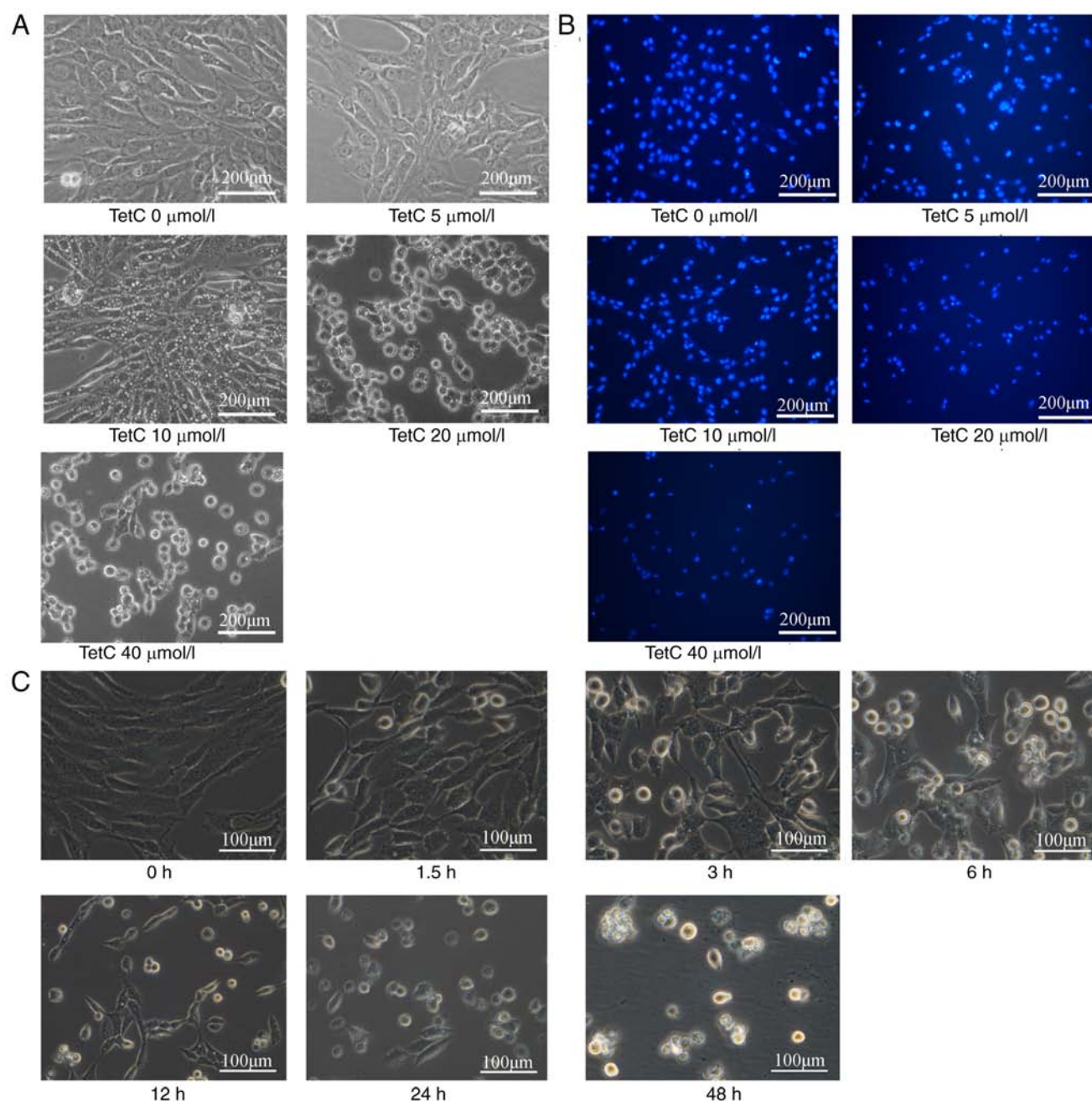


Figure 3. Effect of TetC on intracellular vacuolization and apoptosis in human glioma U87 cells. (A) Cells were treated with 0, 5, 10, 20 and 40 $\mu\text{mol/l}$ TetC for 48 h, and observed under a microscope (x20). (B) Cells were then stained with Hoechst 33342 for 20 min and photographed using a fluorescence microscope (x20). (C) Cells were treated with 20 $\mu\text{mol/l}$ TetC for 0, 1.5, 3, 6, 12, 24 and 48 h and observed under a microscope (x40). TetC, tetrandrine citrate.

were anesthetized by intraperitoneal injection with 10% chloral hydrate (300 mg/kg bodyweight) and were sacrificed by cervical dislocation. When the mice did not move, death was confirmed and then tumor tissues were removed and the body and tumor weights were measured.

Statistical analysis. All experiments were repeated three times. SPSS 17.0 statistical software was used for statistical analysis, and the results are presented as the means \pm standard deviation. Treatment effects were compared using one-way ANOVA and significance was calculated using the LSD test. $P < 0.05$ was considered to indicate a statistically significant difference.

Results

Inhibition of human glioma U87, U251 and HUVEC growth by TetC. The growth-inhibitory effect of TetC on human glioma U87 and U251 cells, in addition to HUVECs, was examined using an MTT assay. The cells were cultured for 24, 48 and 72 h in the presence of 0, 5, 10, 20 or 40 $\mu\text{mol/l}$ TetC. Following treatment with TetC, the proliferative rate of all three cell lines was decreased in a dose-dependent manner (Fig. 2). The IC_{50} values of TetC in U87 cells at 24, 48 and 72 h were 10.4 ± 1.1 , 9.1 ± 0.7 and 7.3 ± 0.6 $\mu\text{mol/l}$, respectively; in U251 cells, the IC_{50} values were 16.6 ± 1.6 (24 h), 12.5 ± 1.2 (48 h) and 10.8 ± 0.9 (72 h) $\mu\text{mol/l}$, and 19.1 ± 1.8 (24 h), 21.3 ± 1.8 (48 h) and 20.3 ± 2.1

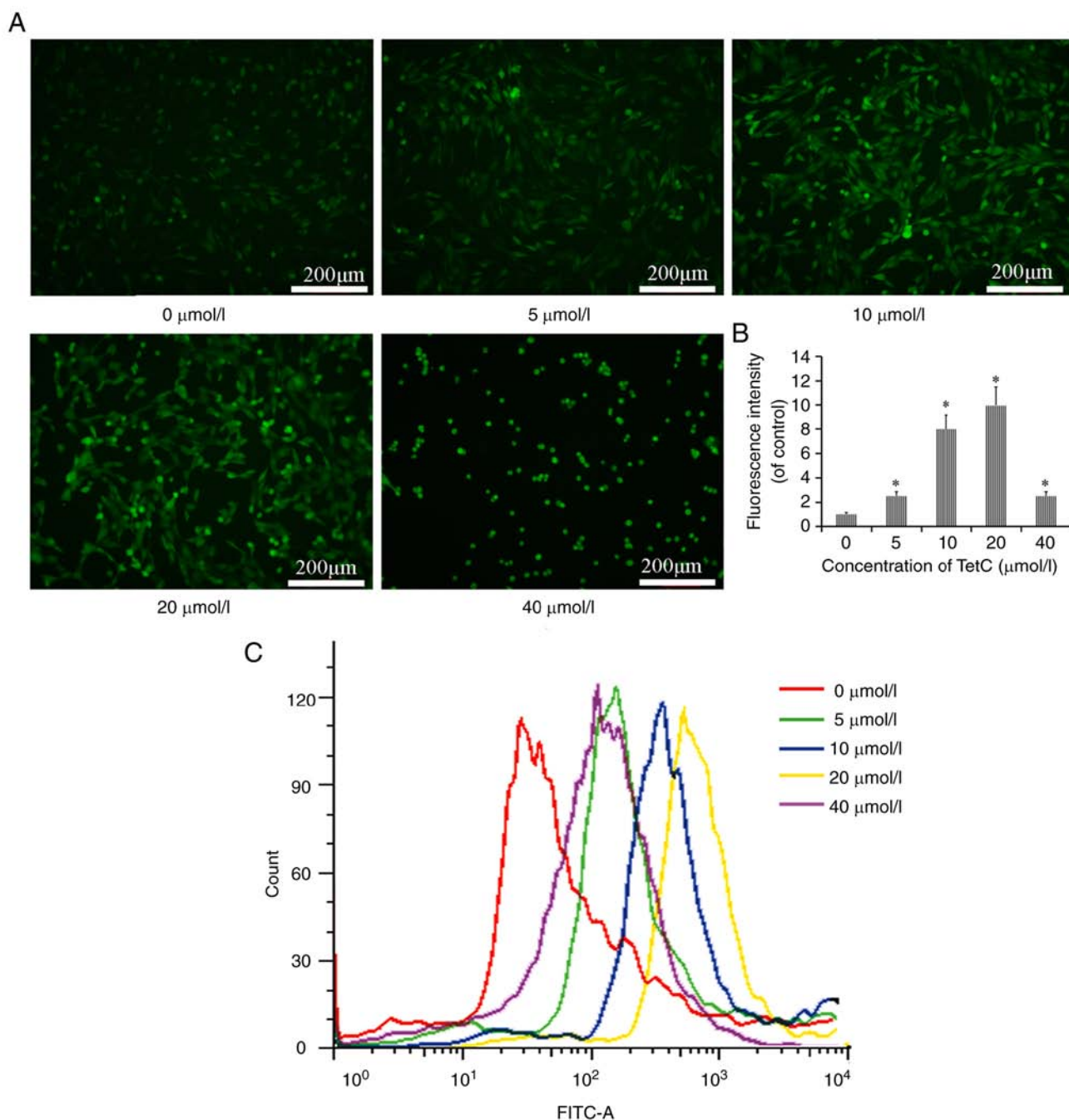


Figure 4. Effect of TetC on the levels reactive oxygen species in U87 cells. (A) Cells were treated with different concentrations of TetC (0, 5, 10, 20 and 40 $\mu\text{mol/l}$) for 48 h and observed under a microscope. (B) Quantification of (A). (C) Following image acquisition, the cells were centrifuged and washed with ice-cold PBS prior to flow cytometric analysis. * $P < 0.05$, compared with the control group. TetC, tetrandrine citrate; ROS, reactive oxygen species.

(72 h) $\mu\text{mol/l}$ in HUVECs. The greatest growth-inhibitory effect was observed in U87 cells, and TetC was more cytotoxic to U87 cells than HUVECs. Therefore, the U87 cell line was selected for use in subsequent experimentation.

TetC induces the vacuolar degeneration of human glioma U87 cells. Human glioma U87 cells were cultured for 48 h in the presence of various concentrations of TetC (0, 5, 10, 20 and 40 $\mu\text{mol/l}$). Cell morphology was then observed by optical microscopy. TetC (10 $\mu\text{mol/l}$) induced the intracellular vacuolization of U87 cells, and ≥ 20 $\mu\text{mol/l}$ induced cell rounding (Fig. 3A). Fluorescence microscopy revealed

that markers of apoptosis, such as nuclear concentration and apoptotic body formation, were induced by ≥ 20 $\mu\text{mol/l}$ TetC (Fig. 3B). In addition, 20 $\mu\text{mol/l}$ TetC induced cell rounding with small vacuole formation in a time-dependent manner (Fig. 3C).

TetC increases ROS production in U87 cells. The effects of TetC on intracellular ROS production in U87 cells were determined using a DCFH-DA fluorescence assay. As revealed in Fig. 4A, the number of fluorescent puncta, representing the concentration of ROS, was higher in TetC-treated cells than in the control cells. In addition, the flow cytometric results

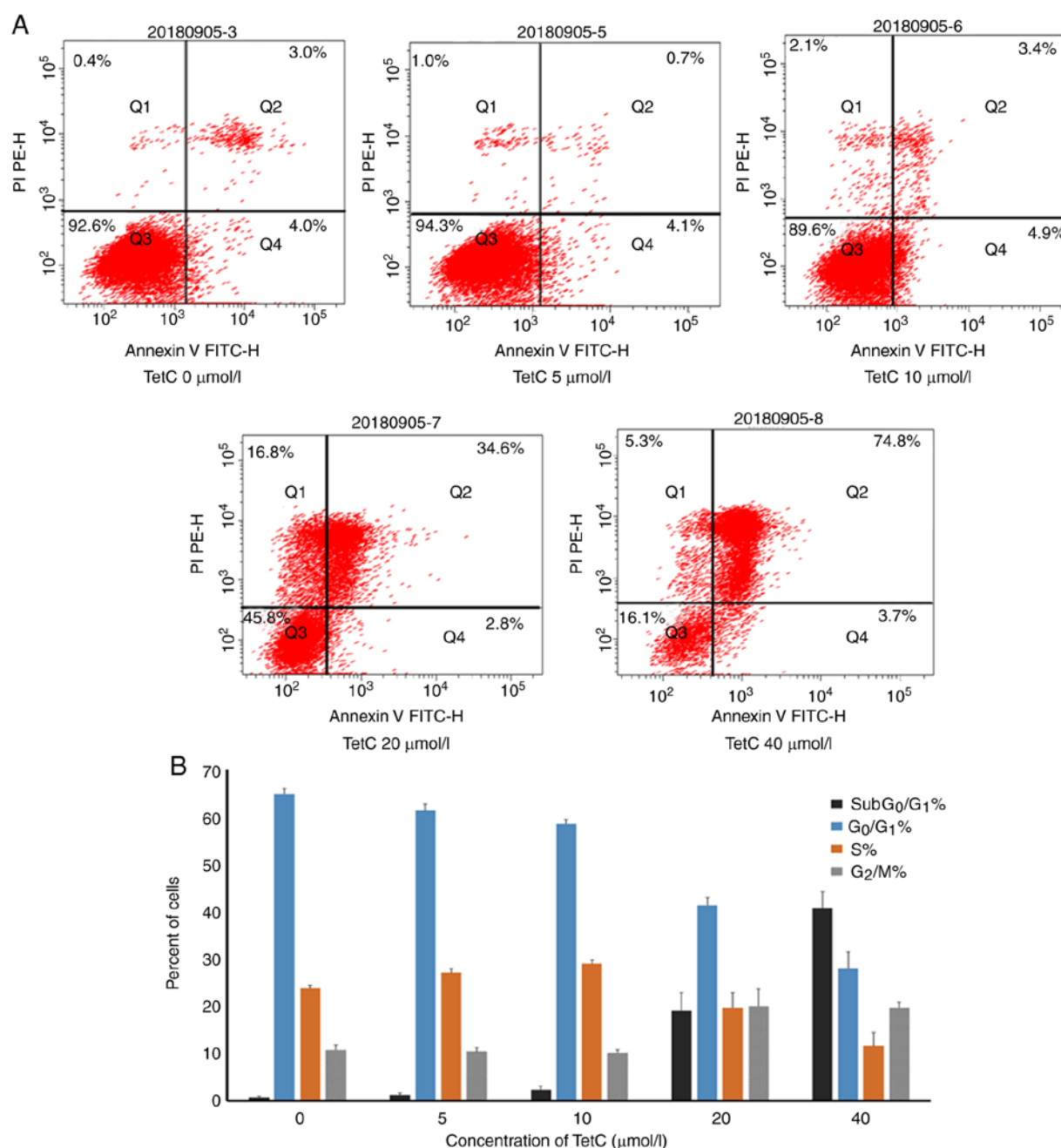


Figure 5. TetC decreases the percentage of cells in the G₀/G₁ phase and induces apoptosis in U87 cells. (A) Cells were treated with different concentrations of TetC (0, 5, 10, 20 and 40 $\mu\text{mol/l}$) for 48 h, and labeled with a combination of FITC-Annexin V and PI, followed by flow cytometric analysis. The percentage of apoptotic cells (upper right (late stage) and lower right quadrants (early stage)) is indicated. (B) Histogram of the cell cycle distribution of U87 cells. TetC, tetrandrine citrate; PI, propidium iodide.

revealed that ROS levels were increased by treatment with 0, 5, 10, 20 and 40 $\mu\text{mol/l}$ TetC, compared with those in the control cells. However, the levels of ROS were increased to a lesser degree following treatment with 40 $\mu\text{mol/l}$, compared with the use of 10 or 20 $\mu\text{mol/l}$ TetC (Fig. 4B and C). These results demonstrated that ROS were produced in U87 cells in response to TetC.

TetC induces U87 cell apoptosis and decreases the percentage of cells in the G₀/G₁ phase. To evaluate the effect of TetC on apoptosis, human glioma U87 cells were treated with different concentrations of TetC. The induction of apoptosis by TetC

was confirmed by FITC-Annexin V/PI staining. The apoptotic ratio was significantly enhanced in cells incubated with 20 or 40 $\mu\text{mol/l}$ TetC for 48 h, compared with that of the control (Fig. 5A). To investigate the effect of TetC on the cell cycle, the cells were treated with 0-40 $\mu\text{mol/l}$ TetC, which significantly altered the cell cycle distribution in a dose-dependent manner; the percentage of the G₀/G₁ phase cells was decreased, and the percentage of cells in the G₂/M and subG₀/G₁ phases was increased (Fig. 5B).

TetC regulates the expression of tumor-related genes in U87 cells. To investigate the mechanisms of TetC in human glioma

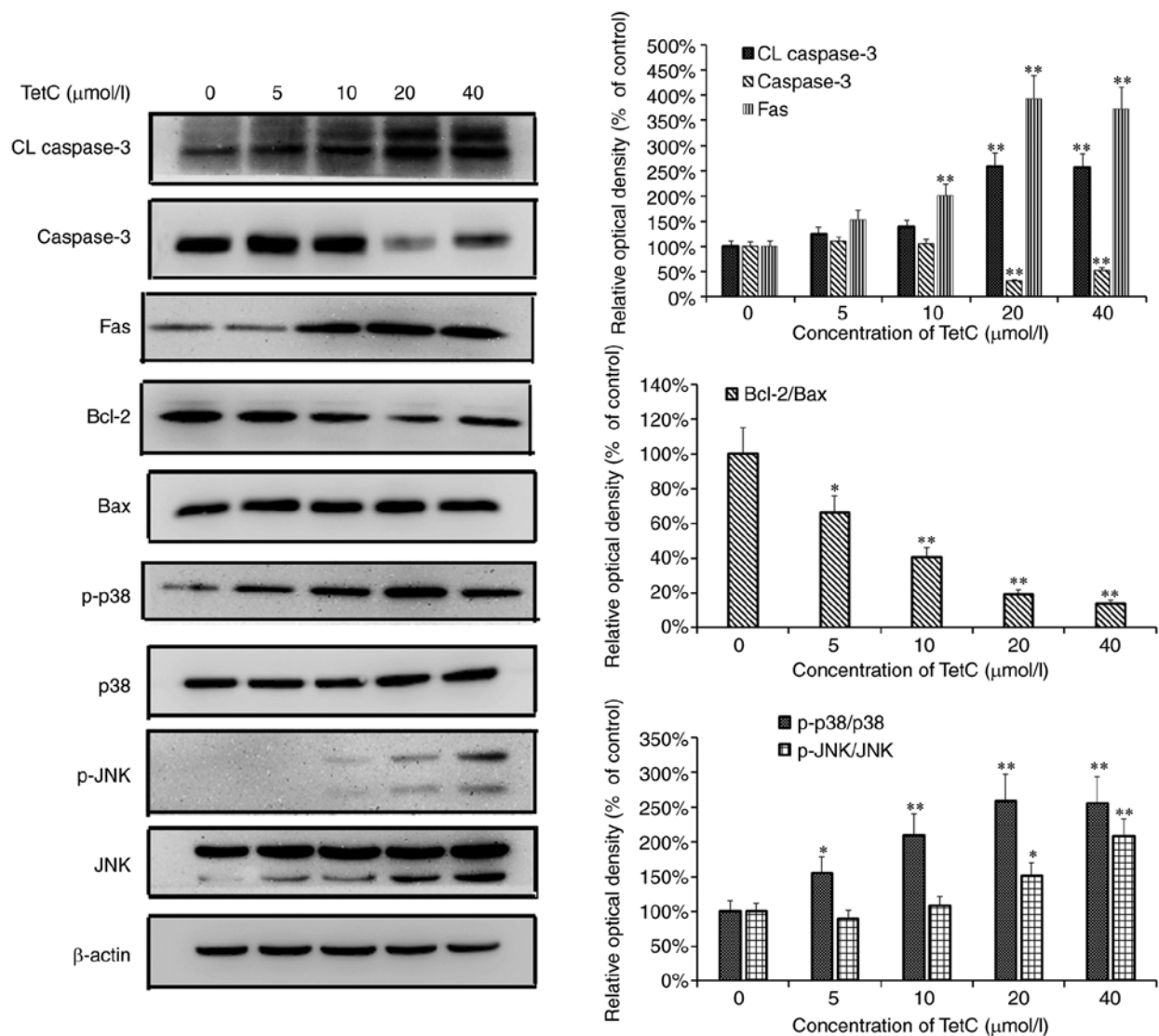


Figure 6. Effect of TetC on the expression levels of apoptosis-associated proteins. Cells were treated with different concentrations of TetC (0, 5, 10, 20 and 40 μ mol/l) for 48 h, and then lysed and subjected to western blotting (three replicates). * P <0.05, and ** P <0.01, compared with the control group. TetC, tetrandrine citrate.

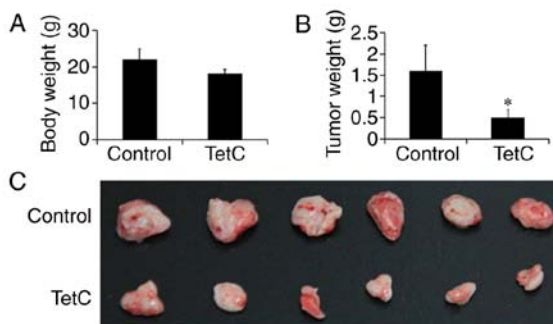


Figure 7. Effects of TetC on the growth of human glioma U87 xenografts in BALB/c nude mice. Following tumor implantation, each animal was intraperitoneally administered 200 μ l PBS (vehicle control) or TetC (200 mg/kg) every other day for 14 days. * P <0.05, compared with the control group. (A) Body weight. (B) Tumor weight. (C) Representative tumor images. TetC, tetrandrine citrate; PBS, phosphate-buffered saline.

revealed in Fig. 6, the expression levels of caspase-3 and Bcl-2 in U87 cells were markedly downregulated following TetC treatment in dose-dependent manner, whereas the levels of CL caspase-3, Fas, p-p38 and p-JNK were increased.

Inhibition of human glioma U87 xenograft growth in BALB/c nude mice. TetC treatment was initiated three days after tumor implantation. TetC was intraperitoneally administered at a dose of 200 mg/kg, every other day for 14 days; the control mice were administered PBS (vehicle only). The body weights of the animals in the control and TetC-treated groups were not significantly different (Fig. 7A), although tumor growth in the TetC-treated BALB/c nude mice was significantly suppressed compared with that in the control mice (Fig. 7B and C). Compared with the control group (1.8 ± 0.11 cm), the maximum diameter of tumors (0.8 ± 0.06 cm) in TetC-treated groups was shorter and there was only one tumor per mouse. Treatment with TetC inhibited the growth of human glioma U87 xenografts by up to 68.7%, which suggests that TetC, at a well-tolerated dose, markedly inhibits U87 xenograft growth.

U87 cells, the effects of TetC treatment on the expression levels of apoptosis-associated proteins were investigated. As

Discussion

Malignant glioma is among the neoplasms with the highest mortality rates, and is associated with one of the worst 5-year overall survival rates among all human cancers (31). Although TMZ has consistently been demonstrated to effectively prolong the survival time of patients with brain tumors, under certain conditions, glioma cells exhibit marked resistance to TMZ (4-6). Therefore, new therapeutic compounds and treatment approaches are required to prolong the survival time of glioma patients. In the present study, the effect of TetC on cell proliferation was investigated using an MTT assay, which revealed that TetC inhibited the proliferation of U87 and U251 cells, as well as HUVECs, in a dose-dependent manner (Fig. 2). Furthermore, these growth-inhibitory effects were most prominent in U87 cells, and a greater cytotoxic effect was apparent in these cells, compared with that in HUVECs. It can therefore be deduced that TetC has a more pronounced effect on U87 cells; thus this cell line was utilized in subsequent experimentation. In the cell viability assay, the vacuolization of U87 cells was observed in the 10 $\mu\text{mol/l}$ TetC-treated group, however cell-rounding with reduced vacuolization was observed in the 20 and 40 $\mu\text{mol/l}$ treatment groups. Furthermore, the change of vacuoles over time at 20 $\mu\text{mol/l}$ TetC was also observed (Fig. 3C). Numerous vacuoles of different sizes appeared in each cell, so it was difficult to quantify the number of vacuoles and size under the current experimental conditions. In addition, cell apoptosis would occur with the prolongation of 20 $\mu\text{mol/l}$ TetC treatment time. It was speculated that different mechanisms of action were responsible for the differences in response to 10 $\mu\text{mol/l}$ and ≥ 20 $\mu\text{mol/l}$ TetC treatment. In the 10 $\mu\text{mol/l}$ TetC-treated group, cell vacuolization was an indication of mitochondrial or endoplasmic reticulum denaturation (32), although some researchers consider this to be the result of methuosis (33). In the 20 and 40 $\mu\text{mol/l}$ TetC-treated groups, cell rounding was more likely to be associated with apoptosis. Subsequently, apoptosis was assessed using flow cytometry and Hoechst staining, and the cell cycle status was investigated by flow cytometry alone. The results of these assays demonstrated that TetC induced apoptosis in a dose-dependent manner. Hoechst staining revealed nuclear concentration and apoptotic body formation in the 20 and 40 $\mu\text{mol/l}$ TetC-treated groups. This suggests that following treatment with TetC, apoptosis contributes to the inhibition of U87 cell proliferation, which was supported by the results of the cell cycle assay.

Mitochondria and the production of ROS serve important roles in the induction of apoptosis under physiological and pathological conditions. Notably, mitochondria are both a source and a target of ROS (34). In the present study, it was observed that compared with the vehicle control, TetC treatment resulted in increased ROS production. However, compared with the 10 and 20 $\mu\text{mol/l}$ TetC-treated groups, single-cell fluorescence intensity analysis revealed that 40 $\mu\text{mol/l}$ TetC decreased the levels of ROS (Fig. 4B), and it was hypothesized that this decrease in fluorescence intensity was the result of apoptosis (Fig. 5). Cell apoptosis leads to the decrease of intracellular ROS. The findings of the 40 $\mu\text{mol/l}$ TetC group in Figs. 4 and 5 were consistent.

Caspase-3 and members of the Bcl-2 protein family act as key regulators of apoptosis, and are important determinants

of cellular sensitivity or resistance to chemotherapeutic drugs (35). Bcl-2 and Bax belong to the Bcl-2 protein family, and Bcl-2 inhibits, whilst Bax promotes apoptosis (36). The present study indicated that although the expression level of Bcl-2 was decreased in a dose-dependent manner, that of Bax, a pro-apoptotic protein, was not significantly altered, thus the Bcl-2/Bax ratio was decreased. Bcl-2 and Bax may therefore be involved in TetC-induced apoptosis. Moreover, an increase in the level of CL caspase-3, but a decrease in the expression level of caspase-3 was observed following TetC treatment; the CL caspase-3/caspase-3 ratio was thus increased. Notably, caspase-3 activation was demonstrated to occur after treatment with TetC. These events have been associated with a decrease in the Bcl-2/Bax ratio (37). In addition, the reason why CL caspase-3 was induced in the control group may be due to too many cells in the control group, which causes apoptosis in few cells. Further research will be performed on this phenomenon.

The JNK and p38 mitogen-activated protein kinase (MAPK) pathways are critical to MAPK signaling. The activation of JNK and p38 MAPK signaling is involved in the initiation of apoptosis by different stimuli in a number of common malignant tumors (38). Therefore, the effect of TetC on the expression and phosphorylation of JNK and p38 MAPK was also investigated. As revealed in Fig. 7, in U87 cells treated with TetC for 48 h, the protein levels of p-JNK and p-p38 MAPK were significantly increased in a dose-dependent manner, compared with those in the control cells. The increased activities of both of these pathways may induce U87 cell apoptosis and thereby inhibit tumor cell growth.

In vivo, it was determined that TetC decreased tumor size and inhibited the growth of human glioma U87-cell xenografts in BALB/c nude mice, without influencing body weight. This result suggests that TetC not only inhibits tumor growth, but is also well tolerated. The limitation of this study is that it is not clear whether TetC can pass through the blood-brain barrier. It is reported that tetrandrine liposomes could pass through blood-brain barrier (39). If TetC cannot pass the blood-brain barrier, Tet liposomes will be used in a future study. In addition, only the effect of TetC on U87 cell apoptosis was investigated in the present study. It is considered that TetC has a wide range of pharmacological effects which will be addressed in a future study.

In conclusion, TetC induced apoptosis in human glioma U87 cells by decreasing the Bcl-2/Bax ratio and increasing the production of ROS, the CL caspase-3/caspase-3 ratio and JNK and p38 phosphorylation. *In vivo*, TetC was highly effective at inhibiting the growth of human glioma U87 xenografts in BALB/c nude mice, and is therefore a promising candidate for the treatment of human gliomas.

Acknowledgements

We acknowledge the technical assistance and support from Dr Jin Liu for flow cytometric analysis.

Funding

The present study was supported by grants from the National Natural Science Foundation of China (grant no. 81671391), the CAMS Innovation Fund for Medical Sciences (grant

no. 2018-I2M-1-002) and the Beijing Hospital Nova Project (grant no. BJ-2016-033 and BJ-2016-034).

Availability of data and materials

The datasets used and/or analyzed during the current study are available from the corresponding author on reasonable request.

Authors' contributions

YL conceived and designed the experiments. JS and YaZ performed the experiments. YoZ and JC analyzed the data. GH assisted in the western blot analysis and manuscript preparation. YL wrote the manuscript. All authors read and approved the manuscript and agree to be accountable for all aspects of the research in ensuring that the accuracy or integrity of any part of the work are appropriately investigated and resolved.

Ethics approval and consent to participate

All animal experimentation was approved by the Institutional Animal Care and Use Committee of Beijing Hospital.

Patient consent for publication

Not applicable.

Competing interests

The authors declare that they have no competing interests.

References

- Friedman HS, Kerby T and Calvert H: Temozolomide and treatment of malignant glioma. *Clin Cancer Res* 6: 2585-2597, 2000.
- Gao J, Wang Z, Liu H, Wang L and Huang G: Liposome encapsulated of temozolomide for the treatment of glioma tumor: Preparation, characterization and evaluation. *Drug Discov Ther* 9: 205-212, 2015.
- Kawaji H, Tokuyama T, Yamasaki T, Amano S, Sakai N and Namba H: Interferon-beta and temozolomide combination therapy for temozolomide monotherapy-refractory malignant gliomas. *Mol Clin Oncol* 3: 909-913, 2015.
- Yu Z, Xie G, Zhou G, Cheng Y, Zhang G, Yao G, Chen Y, Li Y and Zhao G: NVP-BEZ235, a novel dual PI3K-mTOR inhibitor displays anti-glioma activity and reduces chemoresistance to temozolomide in human glioma cells. *Cancer Lett* 367: 58-68, 2015.
- Wang X, Jia L, Jin X, Liu Q, Cao W, Gao X, Yang M and Sun B: NF- κ B inhibitor reverses temozolomide resistance in human glioma TR/U251 cells. *Oncol Lett* 9: 2586-2590, 2015.
- Tian T, Li A, Lu H, Luo R, Zhang M and Li Z: TAZ promotes temozolomide resistance by upregulating MCL-1 in human glioma cells. *Biochem Biophys Res Commun* 463: 638-643, 2015.
- Dunn-Pirio AM and Vlahovic G: Immunotherapy approaches in the treatment of malignant brain tumors. *Cancer* 123: 734-750, 2017.
- Wu Z, Wang G, Xu S, Li Y, Tian Y, Niu H, Yuan F, Zhou F, Hao Z, Zheng Y, *et al*: Effects of tetrandrine on glioma cell malignant phenotype via inhibition of ADAM17. *Tumour Biol* 35: 2205-2210, 2014.
- Li X, Wu Z, He B and Zhong W: Tetrandrine alleviates symptoms of rheumatoid arthritis in rats by regulating the expression of cyclooxygenase-2 and inflammatory factors. *Exp Ther Med* 16: 2670-2676, 2018.
- Gao LN, Feng QS, Zhang XF, Wang QS and Cui YL: Tetrandrine suppresses articular inflammatory response by inhibiting pro-inflammatory factors via NF- κ B inactivation. *J Orthop Res* 34: 1557-1568, 2016.
- Lai JH: Immunomodulatory effects and mechanisms of plant alkaloid tetrandrine in autoimmune diseases. *Acta Pharmacol Sin* 23: 1093-1101, 2002.
- Miao RM, Fang ZH and Yao Y: Therapeutic efficacy of tetrandrine tablets combined with matriline injection in treatment of silicosis. *Zhonghua Lao Dong Wei Sheng Zhi Ye Bing Za Zhi* 30: 778-780, 2012 (In Chinese).
- Zhang HN, Xin HT, Zhang WD, Jin CJ, Huang SY and Zhang Y: The anti-fibrotic effects of Qidan granule in experimental silicosis. *Zhonghua Yu Fang Yi Xue Za Zhi* 41: 290-294, 2007 (In Chinese).
- Miao RM, Sun XF, Zhang YY, Wu W, Fang ZH, Zhao R, Zhao DK, Qian GL and Ji J: Clinical efficacy of tetrandrine combined with acetylcysteine effervescent tablets in treatment of silicosis. *Zhonghua Lao Dong Wei Sheng Zhi Ye Bing Za Zhi* 31: 857-858, 2013 (In Chinese).
- Zhang TJ, Guo RX, Li X, Wang YW and Li YJ: Tetrandrine cardioprotection in ischemia-reperfusion (I/R) injury via JAK3/STAT3/Hexokinase II. *Eur J Pharmacol* 813: 153-160, 2017.
- Huang P, Xu Y, Wei R, Li H, Tang Y, Liu J, Zhang SS and Zhang C: Efficacy of tetrandrine on lowering intraocular pressure in animal model with ocular hypertension. *J Glaucoma* 20: 183-188, 2011.
- Zhang J, Yu B, Zhang XQ, Sheng ZF, Li SJ, Wang ZJ, Cui XY, Cui SY and Zhang YH: Tetrandrine, an antihypertensive alkaloid, improves the sleep state of spontaneously hypertensive rats (SHRs). *J Ethnopharmacol* 151: 729-732, 2014.
- Yuan B, Yao M, Wang X, Sato A, Okazaki A, Komuro H, Hayashi H, Toyoda H, Pei X, Hu X, *et al*: Antitumor activity of arsenite in combination with tetrandrine against human breast cancer cell line MDA-MB-231 in vitro and in vivo. *Cancer Cell Int* 18: 113, 2018.
- N B and K RC: Tetrandrine and cancer-an overview on the molecular approach. *Biomed Pharmacother* 97: 624-632, 2018.
- Wong V, Zeng W, Chen J, Yao XJ, Leung ELH, Wang QQ, Chiu P, Ko BCB and Law BYK: Tetrandrine, an activator of autophagy, induces autophagic cell death via PKC- α inhibition and mTOR-dependent mechanisms. *Front Pharmacol* 8: 351, 2017.
- Liu T, Liu X and Li W: Tetrandrine, a Chinese plant-derived alkaloid, is a potential candidate for cancer chemotherapy. *Oncotarget* 7: 40800-40815, 2016.
- Joshi P, Vishwakarma RA and Bharate SB: Natural alkaloids as P-gp inhibitors for multidrug resistance reversal in cancer. *Eur J Med Chem* 138: 273-292, 2017.
- Fu L, Liang Y, Deng L, Ding Y, Chen L, Ye Y, Yang X and Pan Q: Characterization of tetrandrine, a potent inhibitor of P-glycoprotein-mediated multidrug resistance. *Cancer Chemother Pharmacol* 53: 349-356, 2004.
- Jin L, Xu M, Luo XH and Zhu XF: Stephania tetrandra and ginseng-containing chinese herbal formulation NSEN1 reverses cisplatin resistance in lung cancer xenografts. *Am J Chin Med* 45: 385-401, 2017.
- Chen Y and Tseng SH: The potential of tetrandrine against gliomas. *Anticancer Agents Med Chem* 10: 534-542, 2010.
- Chen Y, Chen JC and Tseng SH: Tetrandrine suppresses tumor growth and angiogenesis of gliomas in rats. *Int J Cancer* 124: 2260-2269, 2009.
- Chang KH, Chen ML, Chen HC, Huang YW, Wu TY and Chen YJ: Enhancement of radiosensitivity in human glioblastoma U138MG cells by tetrandrine. *Neoplasia* 46: 196-200, 1999.
- Imoto K, Takemura H, Kwan CY, Sakano S, Kaneko M and Ohshika H: Inhibitory effects of tetrandrine and hernandezine on Ca²⁺ mobilization in rat glioma C6 cells. *Res Commun Mol Pathol Pharmacol* 95: 129-146, 1997.
- Shi Z, Liang YJ, Chen ZS, Wang XW, Wang XH, Ding Y, Chen LM, Yang XP and Fu LW: Reversal of MDR1/P-glycoprotein-mediated multidrug resistance by vector-based RNA interference in vitro and in vivo. *Cancer Biol Ther* 5: 39-47, 2006.
- Lin YJ and Zhen YS: Rhein lysinate suppresses the growth of breast cancer cells and potentiates the inhibitory effect of Taxol in athymic mice. *Anticancer Drugs* 20: 65-72, 2009.
- Tykocki T and Eltayeb M: Ten-year survival in glioblastoma. A systematic review. *J Clin Neurosci* 54: 7-13, 2018.
- Liu J, Zhen YZ, Cui J, Hu G, Wei J, Xu R, Tu P and Lin YJ: Dynamic influence of Rhein lysinate on HeLa cells. *Int J Oncol* 53: 2047-2055, 2018.
- Li Z, Mbah NE, Overmeyer JH, Sarver JG, George S, Trabbic CJ, Erhardt PW and Maltese WA: The JNK signaling pathway plays a key role in methuosis (non-apoptotic cell death) induced by MOMIPP in glioblastoma. *BMC Cancer* 19: 77, 2019.

34. Gruia MI, Negoita V, Vasilescu M, Panait M, Gruia I, Velescu BS and Uivarosi V: Biochemical action of new complexes of ruthenium with quinolones as potential antitumor agents. *Anticancer Res* 35: 3371-3378, 2015.
35. Hu XH, Zhao ZX, Dai J, Geng DC and Xu YZ: MicroRNA-221 regulates osteosarcoma cell proliferation, apoptosis, migration, and invasion by targeting CDKN1B/p27. *J Cell Biochem* 120: 4665-4674, 2019.
36. Driak D, Dvorska M, Bolehovska P, Svandova I, Novotny J and Halaska M: Bad and Bid-potential background players in preneoplastic to neoplastic shift in human endometrium. *Neoplasma* 61: 411-415, 2014.
37. Ye Y, Zhi F, Peng Y and Yang CC: MiR-128 promotes the apoptosis of glioma cells via binding to NEK2. *Eur Rev Med Pharmacol Sci* 22: 8781-8788, 2018.
38. Lee JY and Yune TY: Ghrelin inhibits oligodendrocyte cell death by attenuating microglial activation. *Endocrinol Metab (Seoul)* 29: 371-378, 2014.
39. Li XT, Tang W, Xie HJ, Liu S, Song XL, Xiao Y, Wang X, Cheng L and Chen GR: The efficacy of RGD modified liposomes loaded with vinorelbine plus tetrandrine in treating resistant brain glioma. *J Liposome Res* 29: 21-34, 2019.



This work is licensed under a Creative Commons Attribution-NonCommercial-NoDerivatives 4.0 International (CC BY-NC-ND 4.0) License.